Flexible Wearable Antenna Based on AMC with Different Materials for Bio-Telemetry Applications

Yara A. Kamel[1, *], Hesham A. Mohamed[1], Hala ELsadek[1], and Hadia M. ELhennawy[2]

[1]*Microstrip Circuits Department, Electronics Research Institute (ERI), Egypt*
[2]*Electronics and Communication Engineering Department, Ain Shams University, Egypt*

ABSTRACT: In this work, a low-profile and flexible antenna operating in the ISM (2.4–2.4835) GHz band for bio-telemetry applications is presented. This antenna is designed on two flexible substrate materials: Roger RO3003 with a thickness of 0.254 mm and jeans fabric material with a thickness of 0.7 mm, of an overall foot print of $20 \times 30 \, \text{mm}^2$. The deformation bending of the designed antenna in two different cases is studied. The designed antenna is backed by a 3×3 artificial magnetic conductor (AMC) array structure, which resulted in the final design configuration. The antenna is backed by an AMC array structure to achieve a lower specific absorption rate (SAR) as well as high gain when it is mounted on biological tissue. For validation, the antenna is fabricated on two flexible substrate materials and then measured in free space as well as on four different parts of the realistic human (chest, back, arm, and leg) body with and without AMC structure. Furthermore, the SAR is measured on cSAR3D flat. Finally, for reliable communication, the link margin is calculated.

1. INTRODUCTION

Recently, wearable devices have attracted a lot of interest due to their ability to be worn on different parts of the patient's body, e.g., the abdomen, arm, back, and chest, for bio-telemetry applications [1–3]. These devices assist in tracking and monitoring the real-time physiological information, such as glucose level [4] and interacranial pressure [5], of the wearer continuously and then transmitting this information to the remote station [6]. Experts and physicians analyze this information, which helps in detecting abnormal situations at an early stage and saving the wearer's life [7]. There are two ways to transfer the wearer's physiological information to remote devices. One sends the data at a close distance, which is called on-body communication. The other sends data to external station, which is called off-body communication [8]. Thus, the crucial component of the wearable devices is the wearable antenna [9–12]. In contrast to antennas working in free space, the performance of the wearable antenna, such as radiation characteristics, gain, and reflection coefficients, is influenced by the presence of human biological tissue as a result of its high permittivity nature. Thus, several factors should be considered when wearable antennas are designed. First, a wearable antenna with a low profile, conformal to the biological tissue, and designed with flexible materials is highly recommended to be comfortable and easy to wear. The textile [12], late [13], polyster film [14], and papers [15, 16] are used as flexible materials for instant. A textile material is preferred in designing wearable antennas because it is a soft, comfortable material and can be integrated with the wearer's clothes. In [17], a triangular patch antenna operating at 5.8 GHz was printed on textile substrate material. Although three shorting pins were added between the patch

and ground plane for increasing the efficiency of an on-body case and broadband response, the design complexity increased, hardening the antenna manufacturing and usability for wearable applications occurred. Besides, the antenna radiation efficiency in free space was only 75%. A wearable antenna fabricated on felt substrate material with dimensions of $(60 \times 60 \times 2) \, \text{mm}^3$ operating in the ISM band was introduced in [10]. This antenna was designed with a narrow impedance bandwidth (BW) feature. In [18], a flexible polyethylene terephthalate (PET) film was used as a substrate of the antenna with a large footprint of $45 \times 40 \, \text{mm}^2$. However, the antenna was not suitable for integrating with clothes for human comfort. Second, the coupling with the lossy biological tissue causes radiation degradation and frequency detuning [19]. Moreover, the absorption of the electromagnetic (EM) wave by human tissue in the form of energy and heat due to the antenna's backward radiation results in long-term health problems [20]. Hence, the SAR value needs to be within the safety limits [21, 22].

One of the methods used to isolate the biological tissue from the wearable antenna and minimize the SAR value is AMC. The wearable antenna backed by Shieldit Super with a large size operating at 5.5 GHz is proposed in [23]. However, the low gain and low radiation efficiency of 79.9% and 75.7% for off-body and on-body cases, respectively, were achieved. A semi-flexible AMC-integrated wearable antenna with a large size was introduced in [12]. In [14] and [24], the antenna was backed by an AMC. However, a performance of narrow BW is noticed. In [25], Although the proposed antenna was mounted on an electromagnetic band gap (EBG) array, the low gain and narrow BW were exhibited. In [26], the radiation efficiency of the proposed antenna with a metamaterial structure in an on-body case is only 61.3% at 2.45 GHz. Table 1 demonstrates

---

* Corresponding author: Yara A. Kamel (yaraashrafkamel@gmail.com).

TABLE 1. Comparison of a presented antenna with recent literature wearable antennas.

Ref.	Freq. (GHz)	antenna size (mm^2)	Reflector size /Array (mm^2)	BW %	Gain (dBi)
[17]	5.8	50 × 50	-	3.6	4.1
[14]	2.4	135 × 135	35.6 × 35.6 /3 × 3	1.38	7.93
[12]	2.45	32×57	31×31 / 4×4	16	6
[23]	5.5		100× 100	11.8	3.5
[24]	2.45	50× 50	21× 21 /3×3	2.4	4.36
[25]	2.45	20 ×35	40 × 40 /2×2	-	-
	5.8			-	-
This work	2.45	20×30	28×28 / 3×3	12	8.12
		20 × 30	28 × 28 /3 × 3	5.3	5.37

the difference between the designed wearable antenna and the previous literature. As observed, the main merits of our design are a smaller antenna, AMC-backed structure, high gain, and wide BW.

In this work, a flexible wearable antenna integrated with Rogers material as well as jeans fabric material working at 2.45 GHz is introduced for bio-telemetry applications. These substrates are chosen due to their flexibility and conformability in worn scenarios. The compactness of the designed wearable antenna with a coplanar waveguide (CPW) is carried out by using six rectangular slits at the right and left edges and etching central slits from the upper edge of the radiator. Besides, two triangles are cut from the ground plane. Meanwhile, the impedance matching of the designed antenna is enhanced by adjusting two triangle slots on the ground plane. For operating the antenna at the desired frequency, four L-shaped elements are added at the corners of the rectangular patch. As the antenna is designed for wearable applications, it is also analyzed on a cubic model consisting of four layers mimicking human tissue. Then, this antenna is backed by a flexible as well as semi-flexible AMC periodic structure for enhancing the gain, reducing the SAR value, and increasing the impedance BW in off-body and on-body cases. Besides, for verification, the wearable antenna is fabricated on the two flexible substrates and then evaluated when being mounted in four different places on a male body.

2. DESIGN OF ANTENNA METHODOLOGY

2.1. Antenna Design

The front of the designed wearable antenna, which consists of a ground plane, a radiating element, and a 50 Ω-CPW, and side view geometries are presented in Figs. 1(a) and 1(b), respectively. The fabrication process is performed on a single-layer as a result of using CPW to feed the designed wearable

antenna. The gap and line widths of the CPW are chosen to achieve a 50 Ω characteristic impedance [27]. For the miniaturization purposes, the rectangular slits are cut on the edges as well as the center of the designed radiating element of the wearable antenna. Two triangles are etched on the ground plane for enhancing the impedance matching, improving the bandwidth, and increasing the path of the current. The overall size of the designated wearable antenna is 20×30 $(0.16\lambda_0 \times 0.24\lambda_0)$ mm^2. Both flexible materials, Roger RO3003 with a loss tangent $(\tan(\delta)) = 0.0009$, a dielectric constant $(\varepsilon_r) = 3$, and a thickness (h_s) of 0.254 mm, and jeans fabric material with a thickness (h_j) of 0.7 mm and a dielectric constant $(\varepsilon_{rj}) = 1.7$ are used as a substrate for the designated wearable antenna in two different scenarios. These materials are used because of their robustness and flexibility, which are required for patient comfort in biomedical applications, while a copper fabric material with a thickness of 0.17 mm is utilized as a conductive layer in the jeans substrate case. The optimized dimensions of the designated wearable antenna are obtained by the assist of Computer Simulation Technology (CST).
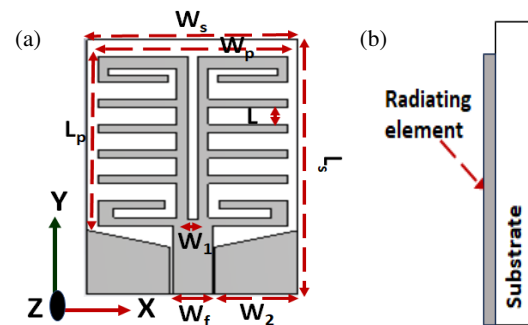
FIGURE 1. (a) Configuration and dimensions of the designed wearable antenna with a dimensions (mm) of $W_s = 20$, $L_s = 30$, $W_p = 20$, $W_1 = 1$, $W_f = 3.7$, $W_2 = 7.9$, $L = 2$, and (b) side view of designated wearable antenna.

2.2. Antenna Design Stages

The desired results are obtained by optimizing the flexible wearable antenna through three successive steps. The design stages along with their reflection coefficients are shown in Figs. 2(a) and 2(b), respectively. As depicted in step 0, the designed antenna is initially based on monopole geometry.
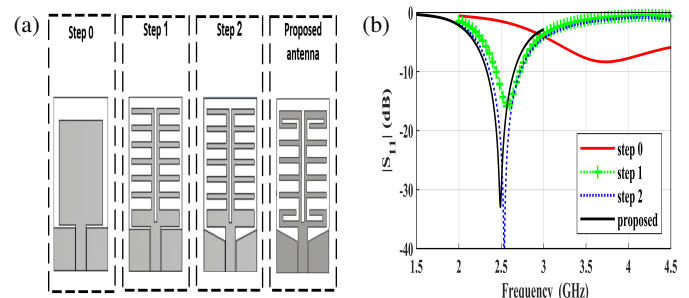
FIGURE 2. (a) Designed wearable antenna evolution, (b) corresponding S_{11} for each stage.

c represents the light speed, f_0 the operating frequency, L_{eff} the effective length, L the length, ΔL the extended length of the patch element, and W the width. For shifting the frequency down, six pairs of horizontal rectangular slits and a vertical rectangular slit are etched on the right and left edges and the upper edge of the rectangular radiating element, respectively, as depicted in step 1. As shown in Fig. 2(b), the resonant frequency is shifted down from 3.7 to 2.59 GHz. Two triangles are cut from the ground plane in order to enhance the impedance matching, improve operating bandwidth, and increase the current path, as demonstrated in step 2. Finally, four L-shaped elements are added to the four corners of the radiating patch element for operating frequency detuning in the ISM band (2.45 GHz), as depicted in step 3 (proposed antenna).

In order to better recognize each step, the current distribution of the proposed wearable antenna is plotted, as depicted in Fig. 3. As shown, the current is concentrated near the CPW feedline in the conventional monopole structure. Since the design of a wearable antenna operating in the ISM band is our target without needing to increase its physical dimension, expanding the current path for shifting the frequency down is required. From Fig. 3, step 1, most of the current is condensed around the six pairs of horizontal slits, followed by the vertical one at the center of the radiating patch. Besides, by adding four L-shaped elements to the radiating patch and cutting two triangular elements from the ground plane, as demonstrated in steps 2 and 3, the deflection of the current and lengthening of its path occur. Hence, the designed wearable antenna operates at the desired ISM frequency band with good impedance matching. As the currents on the two sides of the 50 Ω-CPW flow in the same directions, a CPW line operates in even mode.
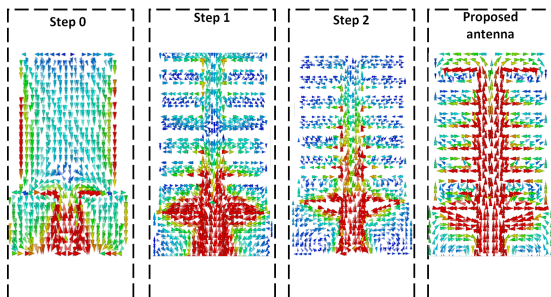
FIGURE 3. Current distribution of the designed wearable antenna for each stage.

3. ANALYSIS OF THE WEARABLE ANTENNA IN FREE SPACE AND ON BIOLOGICAL TISSUE

3.1. Performance of the Designed Antenna in Free Space

The comparison between the performance of the proposed wearable antenna when it is simulated on different substrate materials is depicted in Fig. 4. The proposed wearable antenna is fabricated on Roger as well as jeans fabric substrate materials. In the second case, copper fabric is used as a conductor layer. As shown, a slight shift in the operating frequency between the two different cases is observed. The impedance BWs

of the designed wearable antenna are 13.2% (2.32–2.65) GHz and 17.9% (2.23–2.67) GHz for Roger and textile with copper fabric material, respectively.

Figure 5 illustrates the radiation performance of the designed antenna on Roger and jeans fabric substrates in free space in the XZ and YZ planes. As observed, the omnidirectional pattern is evident. The simulated realized gain of the antenna on the Roger substrate material is 1.8 dBi, while it is 0.95 dBi in the case of the jeans fabric substrate at 2.45 GHz. The radiation efficiency of the proposed wearable antenna is 97% and 80% for two different substrates.
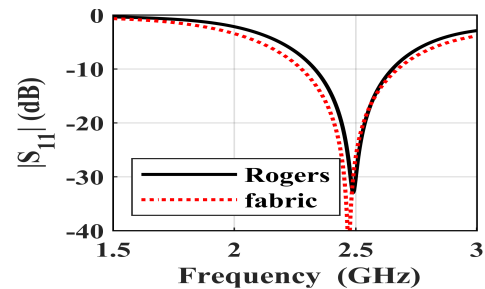
FIGURE 4. Designed wearable antenna with different substrate materials.
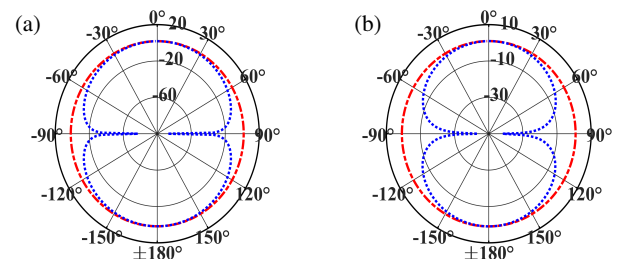
FIGURE 5. RP of wearable antennas in free space for YZ plane (blue line) and XZ plane (red line) on (a) Roger material, and (b) jeans fabric material.

3.2. Bending Analysis of the Proposed Antenna

Deformation of the wearable antenna, such as bending, is expected to occur when the patient wears it or during patient movements. Thus, studying the performance when it bends along the y-axis and x-axis for different bending radii R_y and R_x of 20, 30, 50, and 70 mm is carried out. The impact of bending the designed wearable antenna along the y-axis and x-axis on its performance in the case of Rogers and jeans fabric materials is demonstrated in Fig. 6.

3.3. Biological Tissue

As the wearable antenna is worn on the patient's skin/cloth for the real-time monitoring of physiological data in biomedical applications, the antenna's performance should be examined in the presence of the human body, which is considered as an antenna loading. Therefore, a four-layer phantom consisting of skin, fat, muscle, and bone is constructed with a thickness of 2 mm, 5 mm, 20 mm, and 13 mm for each layer, respectively. Furthermore, For simplicity and reducing the computational time, the cubic phantom has dimensions of $150 \times 150 \times 40$ mm^3.
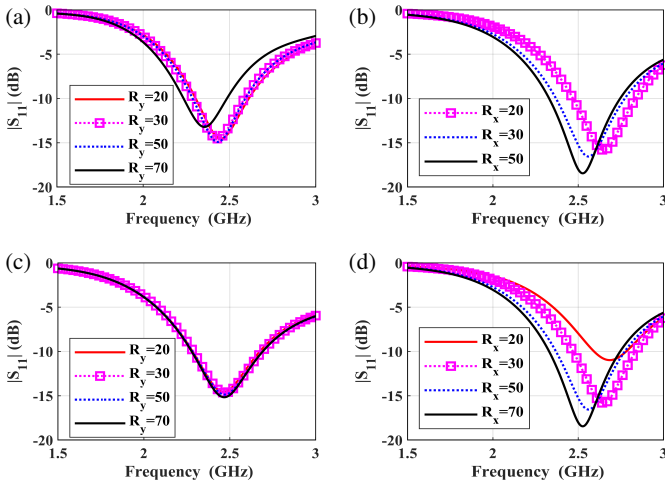
FIGURE 6. Performance of the bending-designed antenna with different radii in an off-body case with (a) Roger material along the y-axis, (b) Roger material along the x-axis, (c) jeans fabric material along the y-axis, and (d) jeans fabric material along the x-axis.

This cubic model is widely used for assisting the analysis of wearable antennas [28]. As the biological tissue is frequency-dependent, the Cole-Cole dispersive model is chosen for estimating the complex permittivity $\varepsilon(\omega)$ of each layer, which is given by [29–31]

$$\varepsilon_r(\omega) = \varepsilon_\infty + \sum_n \frac{\Delta\varepsilon_n}{1 + (j\omega\tau)^{(1-\alpha_n)}} + \frac{\sigma_i}{j\omega\varepsilon_0} \qquad (1)$$

where ε_∞ represents the permittivity of the upper frequency, τ the relaxation time, $\Delta\varepsilon_n$ the dispersion magnitude, α_n the exponent, and σ_i the conductivity.

3.4. Antenna on Human Tissue

As mentioned, the designed wearable antenna is mounted on the cubic model with a separation distance d from the skin layer for examining its performance. To evaluate the influence of the gap distance on the performance of the designed antenna, the reflection coefficient S_{11} is simulated when gap distance varies from 1 to 4 mm, as demonstrated in Figs. 7(a) and 7(b). As shown, the operating frequency of the designed wearable antenna is shifted up, and impedance matching is enhanced with
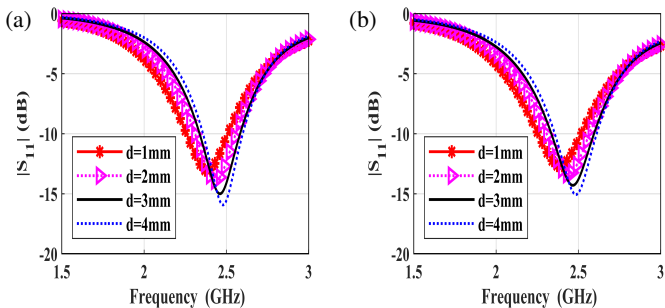
the increase of the separation distance. This demonstrates that the antenna's performance is improved when the separation between the designed antenna and the skin increases [32].

Furthermore, the simulated realized gain of the designed wearable antenna on the human tissue in the XZ and YZ planes at 2.45 GHz for the different two cases is introduced in Fig. 8. As shown, the realized gain at the separation distance of 3 mm is -0.469 dBi and -1.02 dBi for the two planes with a broadside direction, respectively. Besides, a worsening of the simulated gain value of the proposed wearable antenna is observed as the gap distance decreases. Thus, to overcome these drawbacks mentioned above as a result of loading the antenna on biological tissue, the AMC is introduced as a ground plane.
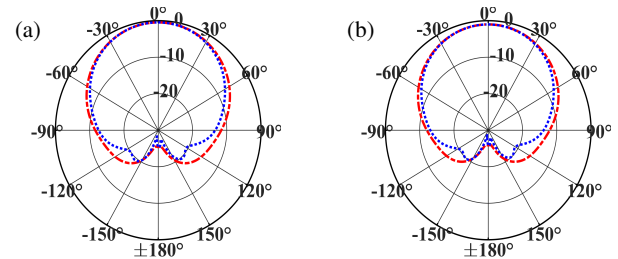
FIGURE 8. RP of wearable antennas on biological tissue for YZ plane (blue line) and XZ plane (red line) on (a) Roger material, and (b) jeans fabric material.

3.5. AMC Design

As the wearable antenna is mounted on the human body in this application, reducing the back radiation, which is harmful to the human body, and enhancing the proposed antenna gain are essential requirements [33]. Thus, the AMC is introduced as a ground plane at a distance much less than $\lambda_0/4$, which assists in the size reduction without impacting the antenna's performance [34, 35] for isolating it from the biological tissue. This is a result of the fact that the AMC acts as a perfect magnetic conductor (PMC), which does not exist in nature. The PMC has zero phase reflection for the incident plane wave, which leads to constructive interference. Therefore, the original antenna's current and its image will be in the same direction as the existence of the AMC.

A simple square loop AMC with full ground is designed, as depicted in Fig. 9(a). The overall size of the AMC unit cell is

FIGURE 7. (a) performance of the designed antenna with a Roger material on the tissue, and (b) performance of the designed antenna with a fabric material on the tissue.
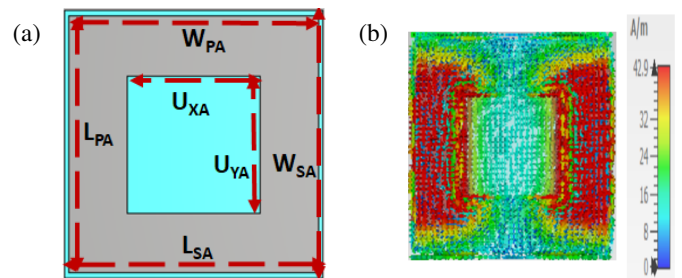
FIGURE 9. (a) Geometry of an AMC unit cell with dimensions of $W_{SA} = L_{SA} = 28$ mm, $W_{PA} = W_{PA} = 27$ mm, $U_{XA} = U_{YA} = 14.4$ mm, and (b) surface current of the AMC unit cell at the desired frequency.

28×28 $(0.22\lambda_0 \times 0.22\lambda_0)$. 1.52 mm-thick semi-flexible Roger RO5880 and 0.7 mm-thick jeans fabric material are employed as substrates for the designed AMC. The operating frequency of the designed AMC can be calculated using the equation [36]

$$f_r = \frac{1}{2\pi\sqrt{LC}} \qquad (2)$$

where f_r presents the operating frequency, L a inductance, and C the capacitance. As observed from Equation (2), the resonance frequency is shifted up with decreasing the capacitance or inductance of the AMC unit cell. This is recognized by displaying the surface current at 2.45 GHz. As demonstrated in Fig. 9(b), the current distribution is concentrated over the square loop. Besides, by comparing the square patch AMC unit cells with and without a square slot, the two cases introduced in-phase reflection at the resonant frequencies of 3.07 GHz and 2.45 GHz, respectively, as shown in Fig. 10. Thus, a symmetric square slot is cut for size reduction of the AMC unit cell by increasing the effective capacitance, which helps in shifting the reflection phase to the lower frequency. The dimensions U_{XA} and U_{YA} of the square slot are optimized to 20.8 mm in the case of using jeans fabric as the antenna's substrate for introducing the zero phase at 2.454 GHz. As depicted, the reflection phase changes from $+180°$ to $-180°$ versus the frequency. The AMC geometry acts as a PMC at the operating frequency of 2.45 GHz with $+90°$ to $-90°$ bandwidth. On the other hand, it acts as perfect electric conductor (PMC) from $+180°$ to $+90°$ and $-90°$ to $-180°$ [37].
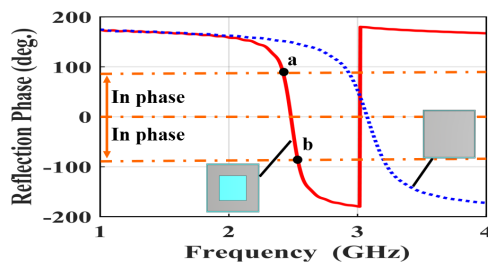
FIGURE 10. Reflection phase of the AMC unit cell.

3.6. Antenna Performance When Integrated with AMC and PEC in an Off-Body Case

The study is performed when the designed antenna is positioned over a 3×3 AMC periodic structure and then compared when it is positioned on PEC with the same dimensions of AMC unit cells for comparison purposes in an off-body case. The designed wearable antenna is placed above the AMC periodic structure and PEC at a separation distance less than $\lambda_0/6$ for size reduction. The total dimensions of the AMC periodic structure are $84 \times 84\,\text{mm}^2$ ($0.68\lambda_0 \times 0.68\lambda_0\,\text{mm}^2$). As a result of mutual impedance coupling between the designed antenna and the AMC periodic structure, frequency detuning and poor impedance matching occur. Thus, the dimensions of the hypotenuse of the two etched triangles on the ground plane are optimized to be 1 mm and 0.5 mm instead of 2 mm in the absence of the AMC case for enhancing impedance matching and

assisting in operating the antenna at the desired frequency in the case of both Rogers and jeans fabric substrates, respectively.

Furthermore, for analyzing a PEC-backed designated wearable antenna, a copper sheet with a conductivity of 5.8×10^7 S/m is placed below a designated antenna. The performance of the designated antenna integrated at a close distance with AMC and PEC reflectors is depicted in Fig. 11. As shown, the reflection coefficient for the designed antenna placed on the PEC is near 0 dB because of the destructive interference with the incident wave [38]. In contrast, good impedance matching is performed when the designated antenna is placed on the AMC structure. The impedance BWs of the the integrated antenna with AMC are 8.3%(2.3–2.5) GHz and 12.3% (2.2–2.49) GHz for Roger and jeans fabric substrates, respectively.
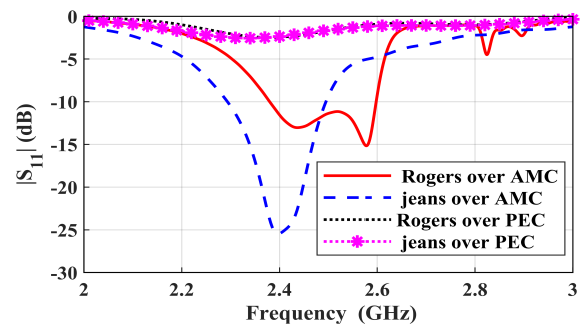
FIGURE 11. Performance of the designed wearable antenna over AMC and PEC in free space.

Besides, the AMC has an impact on enhancing the radiation performance of the designed wearable antenna. By comparing the radiation patterns of the designed antenna with and without AMC array in XZ and YZ planes, the realized gains of the antenna placed on AMC are 7.72 dBi and 4.1 dBi, as shown in Fig. 12, whereas the antenna without AMC, as mentioned above, has 1.8 dBi and 0.95 dBi for Roger and jeans fabric substrates, respectively.
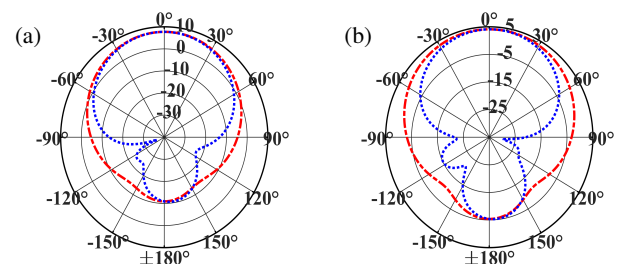
FIGURE 12. RP of wearable antennas over AMC for YZ plane (blue line) and XZ plane (red line) on (a) Roger material, and (b) jeans fabric material.

3.7. Antenna Performance When Integrated with AMC in an On-Body Case

As the antenna is designed for wearing purposes, the designated antenna with AMC is placed on a cubic phantom model, which consists of four layers. This study is performed when the thickness of the worn clothes is taken into consideration as 1 mm,

2 mm, and 3 mm, as well as when the antenna is in direct contact with the cubic phantom mode. As illustrated in Figs. 13(a) and 13(b), the designed wearable antenna placed on AMC in an on-body case has stable performance at different separation distances for the Roger and jeans fabric substrates, respectively. The impedance BWs of the integrated antenna with AMC in an on-body case are 12% (2.3–2.59) and 5.3% (2.3–2.48) GHz for Roger and jeans fabric substrates, respectively.
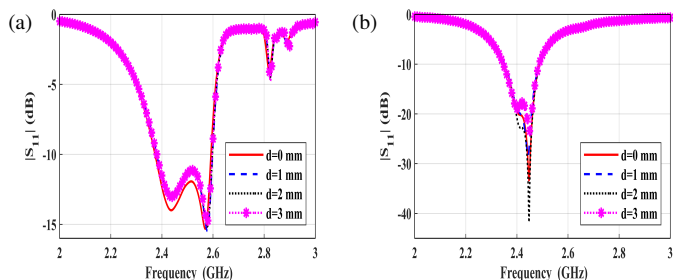
FIGURE 13. (a) performance of the designed antenna over AMC with a Roger material on the tissue, and (b) performance of the designed antenna over AMC with a fabric jeans material on the tissue.

Furthermore, the realized gain of the designed antenna placed on the AMC structure in an on-body is illustrated in Figs. 14(a) and 14(b). As reported, the realized gain is 8.12 dBi and 5.37 dBi for both substrate scenarios in two different planes, respectively. The radiation efficiencies of the proposed antenna with and without an AMC array in an on-body case are 99.2% and 17.3%, respectively, for Rogers substrate, while they are 66.8% and 13.8% for jeans fabric substrate.
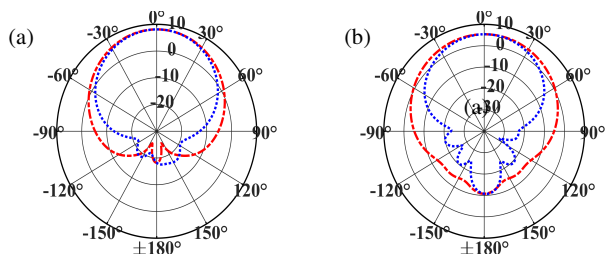
FIGURE 14. RP of wearable antennas over AMC in an on-body case for YZ plane (blue line) and XZ plane (red line) on (a) Roger material, and (b) jeans fabric material.

4. MEASUREMENT RESULTS AND DISCUSSIONS

4.1. Measurement of Jeans Material Dielectric Properties

The dielectric properties of the jeans substrate material used in the fabrication of the wearable antenna is measured using the SPEAGE dielectric assessment kit (DAK) with an open-ended coaxial 3.5 probe, as depicted in Fig. 15(a). As shown, the open-ended coaxial probe is connected to Rohde & Schwarz ZVA67 vector network analyzer (VNA) via flexible cables. The dielectric constant of the material throughout the range of the frequency from 0.5 GHz up to 7 GHz is demonstrated in Fig. 15(b). As the designated antenna is designed to operate in the ISM band, the relative permittivity of the material at 2.45 GHz is 1.2. Depending on this value, the electrical prop-
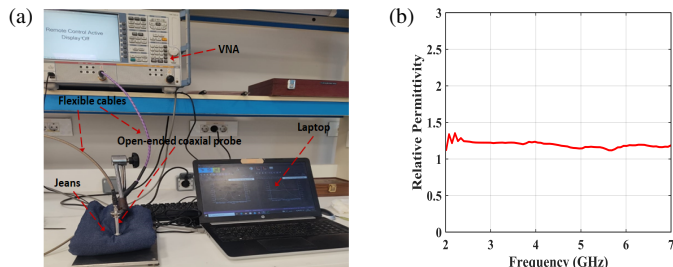
FIGURE 15. (a) The dielectric permittivity measurements setup, and (b) the relative permittivity of the jeans fabric material.

erties of the jeans substrate material are specified in the simulation.

4.2. Free-Space Results

Initially, the designated wearable antenna is etched on flexible substrate materials of Roger RO3003 and jeans fabric with a thickness of 0.254 mm and 0.7 mm, respectively. The fabricated antennas are depicted in Figs. 16(a) and 16(b). For measuring the fabricated antenna's performance, the SMA connector is soldered to the CPW feed line, and then connected to the Rohde & Schwarz ZVA67 VNA, as illustrated in Fig. 17(a). The simulated and measured results of the two fabricated antennas are demonstrated in Fig. 17(b). As observed, the −10 dB impedance BWs of the fabricated wearable antennas on Roger and jeans fabric substrates are 16.5% (2.26–2.67) GHz and 11.7% (2.31–2.6) GHz, respectively.
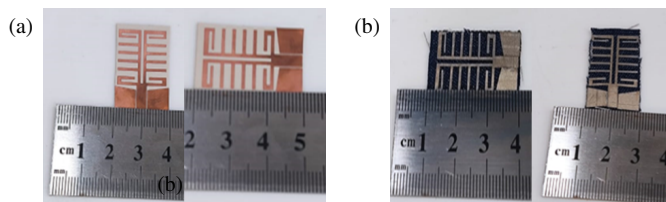
FIGURE 16. Fabricated wearable antenna on (a) Roger material, and (b) jeans fabric material.
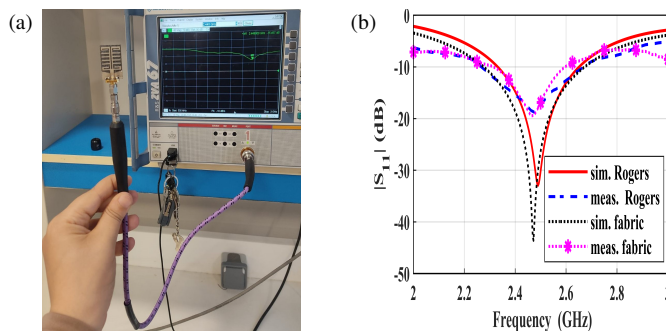
FIGURE 17. (a) Measurement setup of the $|S_{11}|$ of the fabricated antenna on jeans fabric material, and (b) comparison between the simulated and measured antenna performance.

Furthermore, in a real-world environment, wearable antenna bending is predicted. Thus, the bending sensitivity of the fabricated antenna is tested by bending it onto a curve-shaped build-
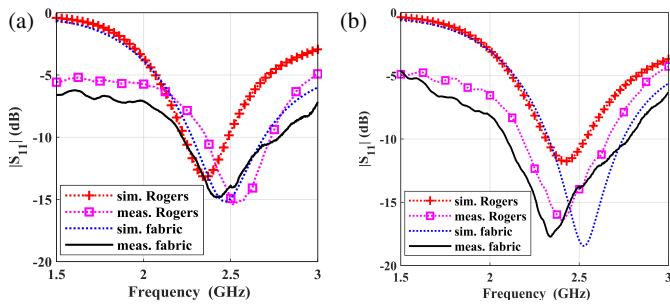
FIGURE 18. (a) simulated and measured $|S_{11}|$ of the fabricated antenna bent along y-axis, and (b) simulated and measured $|S_{11}|$ of the fabricated antenna bent along x-axis.
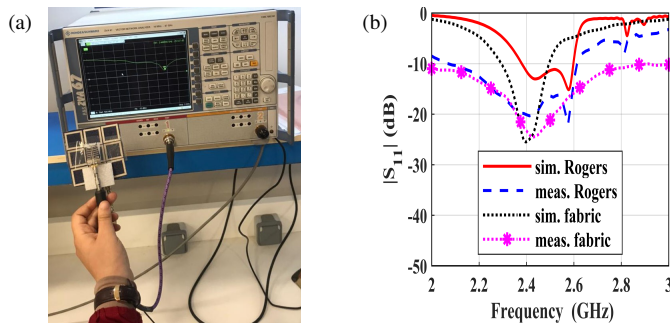
FIGURE 19. (a) Measurement setup of the reflection coefficient of the fabricated antenna on jeans fabric material with AMC, and (b) comparison between the simulated and measured antennas with AMC performance.

FIGURE 20. Comparison between measured (red line) and simulated (blue line) RP of wearable antennas on (a) roger material in XZ plane, (b) roger material in YZ plane, (c) jeans fabric material in XZ plane, and (d) jeans fabric material in YZ plane.

FIGURE 21. (a) The measured S_{11} of the integrated antenna on Roger substrate on four human body parts, and (b) the measured S_{11} of the integrated antenna on jeans fabric substrate on four human body parts.

ing with a styrofoam with a radius of 35 mm. The measured impedance BWs of the antenna fabricated on Roger and jeans fabric substrates along the y-axis and x-axis are depicted in Figs. 18(a) and 18(b).

Comparison between measured and simulated radiation patterns (RPs) of the antenna integrated on Roger and jeans fabric substrate materials is demonstrated in Fig. 20.

These antennas are then integrated with AMC structures and printed on semi-flexible substrate RO5880 with a thickness of 1.52 mm and the same antenna's jeans fabric substrate. The measurement setup of the reflection coefficient of the fabricated antennas placed on the AMC structures is depicted in Fig. 19(a) for jeans fabric substrates. The measured impedance BWs are 23% (2.06–2.61) GHz and 36.06% (2–2.88) GHz of the antenna fabricated on Roger and jeans fabric substrates with AMC structures, respectively.

4.3. On-Body Results

To verify the performance of the designated antenna in the on-body case and study the effect of biological tissue on it, the fabricated antenna performance is tested when it is mounted on a male volunteer. The impedance BWs of the Roger substrate case are 17.3% (2.1–2.5) GHz, 21.2% (2.1–2.6) GHz, 31.1% (<2–2.6) GHz, and 12.2% (2.3–2.6) GHz for placing it on the chest, back, arm, and leg, respectively, as depicted in Fig. 21(a), while the impedance BWs in the jeans fabric substrate case are 26% (2–2.6) GHz, 20.4% (2.2–2.7) GHz, 21.2%

(2.1–2.6) GHz, and 16.6%(2.2–2.6) GHz for the same four parts of the human body, as illustrated in Fig. 21(b).

The prototype wearable antenna integrated with 3×3 AMC array is evaluated by mounting it on the same four male body parts. The impedance BWs of the AMC array integrated wearable antenna with Rogers substrate case are 21.2% (2.1–2.6) GHz, 21.2% (2.1–2.6) GHz, 23.5% (2.06–2.61) GHz, and 26.8% (2–2.62) GHz for the chest, back, arm, and leg, respectively, as reported in Fig. 22(a), while the integrated antenna performance in jeans fabric substrate material case is 21.1% (2.2–2.72) GHz, 21.1% (2.1–2.72) GHz, 25.7% (2.1–2.72) GHz, and 23.2% (2.05–2.59) GHz for the same four realistic male body parts, as demonstrated in Fig. 22(b).

4.4. Safety Consideration

The evaluation of SAR at the operating frequency is the main parameter to ensure patient safety where the human tissue is exposed to the EM wave from the antenna's back radiation. Thus, the SAR level is measured for 1 gm and 10 gm standards when the fabricated wearable antenna is located directly on the cSAR3D flat phantom, which is the worst-case study, as illustrated in Fig. 23(a). As a benchmark, the input power of the
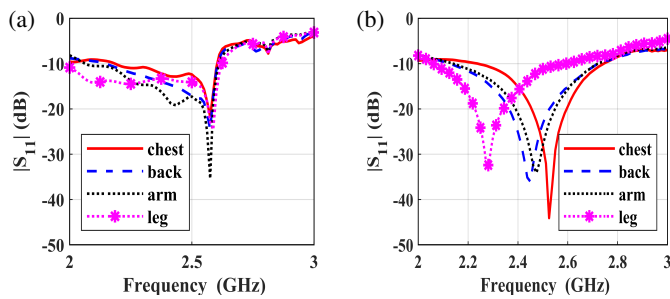
FIGURE 22. (a) The measured S_{11} of the integrated antenna on Roger substrate on four human body parts, and (b) the measured S_{11} of the integrated antenna on jeans fabric substrate on four human body parts.
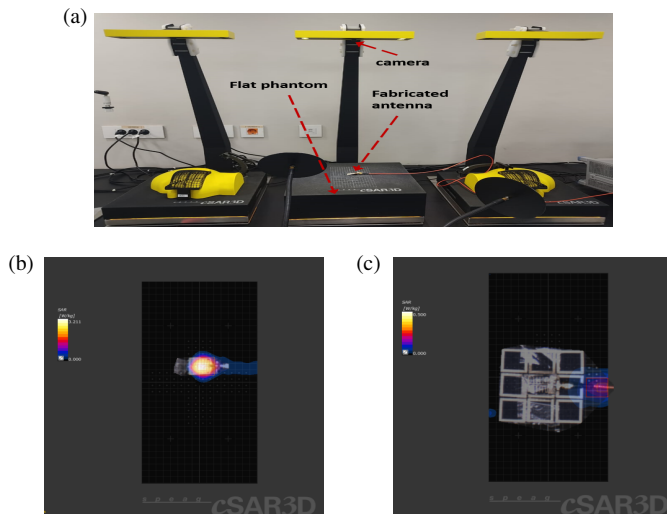
FIGURE 23. (a) cSAR3D phantoms, (b) Measurements the SAR level of the fabricated antenna integrated with fabric material, and (c) Measurements the SAR level of the fabricated antenna integrated with fabric material over the AMC.

fabricated antenna is set to 100 m Watt. The average SAR values corresponding to the 1999 IEEE standard are 2.38 W/kg and 2.38 W/kg for Roger and jeans fabric substrates, respectively. The SAR distribution of the antenna only is depicted in Fig. 23(b). The simulated SAR values are 1.38 W/kg and 1.36 W/kg for Roger and jeans fabric substrates, respectively, while the average SAR values corresponding to the 2005 IEEE standard are 0.98 W/kg and 0.98 W/kg with an input power of 100 m Watt for the same substrate materials while the simulated values are 1.97 W/kg and 1.77 W/kg. According to the SAR values, when the antenna is placed on the phantoms without the AMC structure, these values exceed the safety limits stated by the International Commission on Non-Ionizing Radiation Protection (ICNIRP) and Federal Communications Commission (FCC). Thus, reducing the SAR level to be within the safety limits and ensuring safety considerations are necessary. The SAR field distribution of the fabricated antenna over AMC on a flat phantom is demonstrated in Fig. 23(c). The average SAR values corresponding to the 1999 IEEE standard are 0.142 W/kg and 0.142 W/kg for Roger and jeans fabric substrates, respectively. The simulated SAR values are 0.74 W/kg and 1.2 W/kg for the two substrate materials, while the average SAR values

corresponding to the 2005 IEEE standard are 0.064 W/kg and 0.071 W/kg with an input power of 100 m Watt for the same substrate materials. The simulated SAR values are 0.67 W/kg and 0.48 W/kg for the two substrate materials. As observed, the average SAR values in the presence of the AMC structure are much lower than the standard limits, which ensure the patient safety. Besides, by comparing the simulated and measured SAR values, there are differences between them. This could be attributed to the difference in conductivity and permittivity of the ready phantom material, which are 1.95 S/m and 52.7, respectively.

5. LINK BUDGET EVALUATION

The link budget is evaluated to examine the reliability of the communication between the wearable antenna integrated with the AMC structure on-body (TX) from Section 3.7 and when it is off-body (RX) from Section 3.6. By using the equations in [39], the link margin is evaluated. The required parameters needed for the calculations of the link margin (LM) at 100 kb/s and 1 Mb/s bit rates are listed in the Table [46, Table(IV)] and [40]. The modulation technique used in this work is phase shift keying (PSK). Figs. 24(a) and 24(b) illustrate the link margin versus distance. By considering that the minimum link margin is 20 dB for reliable transferring of the physiological data, the transmitting distance between two antennas can be 301.5 m and 198.4 m for bit rates of 100 kbps in two substrate cases, and the distance will be 95.7 m and 45.2 m for bit rates of 1 Mbps in two substrate cases.
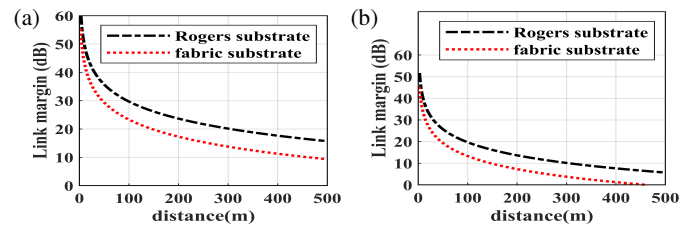
FIGURE 24. Link margin of the wearable antenna placed on AMC for different bit rates (a) 100 kbps, and (b) 1 Mbps.

6. CONCLUSION

In this work, a flexible wearable antenna with CPW-fed work in the ISM band is designed on two different substrate materials for bio-telemetry applications. The designed wearable antenna is studied in free space as well as on a cubic model mimicking the human body, considering the different thicknesses of the worn clothes. It is observed that bad performance occurs when the antenna is placed directly on human tissue as a result of its lossy nature. Thus, 3×3 AMC array integrates a wearable antenna for enhancing the realized gain of the designed antenna as a result of back radiation reduction. The realized gains of the designed antenna integrated on Roger and fabric substrate materials over AMC in an on-body case are 8.12 dBi and 5.37 dBi instead of -0.469 dBi and -1.02 dBi in the absence of the AMC array. Also, the AMC assists in isolating the designed antenna from the biological tissue, which helps in reducing the SAR value below the two standard safety limits.

Thus, the designed antenna is suitable for the use in biomedical applications. The designed antenna was printed on two flexible substrate materials for validation. Then it was measured at different parts of the realistic human body. SAR is measured by locating the antenna on the cSAR3D flat phantom. Finally, the link margin is evaluated for the reliability of the antenna's communication capabilities.

REFERENCES

[1] Seman, F. C., F. Ramadhan, N. S. b. Ishak, R. Yuwono, Z. Z. Abidin, S. H. Dahlan, S. M. Shah, and A. Y. I. Ashyap, "Performance evaluation of a star-shaped patch antenna on polyimide film under various bending conditions for wearable applications," *Progress In Electromagnetics Research Letters*, Vol. 85, 125–130, 2019.

[2] Kamalaveni, A. and M. G. Madhan, "A compact TRM antenna with high impedance surface for SAR reduction at 1800 MHz," *AEU — International Journal of Electronics and Communications*, Vol. 70, No. 9, 1192–1198, 2016.

[3] Aziz, A. A. A., A. T. Abdel-Motagaly, A. A. Ibrahim, W. M. A. E. Rouby, and M. A. Abdalla, "A printed expanded graphite paper based dual band antenna for conformal wireless applications," *AEU — International Journal of Electronics and Communications*, Vol. 110, 152869, 2019.

[4] Liu, L. W., A. Kandwal, Q. Cheng, H. Shi, I. Tobore, and Z. Nie, "Non-invasive blood glucose monitoring using a curved goubau line," *Electronics*, Vol. 8, No. 6, 662, 2019.

[5] Khan, M. W. A., A. Khan, M. Rizwan, L. Sydänheimo, T. Björninen, L. Ukkonen, and Y. Rahmat-Samii, "Loop antenna for deep implant powering in an intracranial pressure monitoring system," in *2018 IEEE International Symposium on Antennas and Propagation & USNC/URSI National Radio Science Meeting*, 207–208, IEEE, 2018.

[6] Hall, P. S. and Y. Hao, *Antennas and Propagation for Body-centric Wireless Communications*, Artech House, 2012.

[7] Chandra, R., H. Zhou, I. Balasingham, and R. M. Narayanan, "On the opportunities and challenges in microwave medical sensing and imaging," *IEEE Transactions on Biomedical Engineering*, Vol. 62, No. 7, 1667–1682, 2015.

[8] Yan, S. and G. A. E. Vandenbosch, "Radiation pattern-reconfigurable wearable antenna based on metamaterial structure," *IEEE Antennas and Wireless Propagation Letters*, Vol. 15, 1715–1718, 2016.

[9] Gao, G.-P., B. Hu, S.-F. Wang, and C. Yang, "Wearable circular ring slot antenna with EBG structure for wireless body area network," *IEEE Antennas and Wireless Propagation Letters*, Vol. 17, No. 3, 434–437, 2018.

[10] Khajeh-Khalili, F., F. Haghshenas, and A. Shahriari, "Wearable dual-band antenna with harmonic suppression for application in medical communication systems," *AEU — International Journal of Electronics and Communications*, Vol. 126, 153396, 2020.

[11] Alemaryeen, A. and S. Noghanian, "On-body low-profile textile antenna with artificial magnetic conductor," *IEEE Transactions on Antennas and Propagation*, Vol. 67, No. 6, 3649–3656, 2019.

[12] Alemaryeen, A. and S. Noghanian, "Crumpling effects and specific absorption rates of flexible amc integrated antennas," *IET Microwaves, Antennas & Propagation*, Vol. 12, No. 4, 627–635, 2018.

[13] Agarwal, K., Y.-X. Guo, and B. Salam, "Wearable amc backed near-endfire antenna for on-body communications on latex substrate," *IEEE Transactions on Components, Packaging and Manufacturing Technology*, Vol. 6, No. 3, 346–358, 2016.

[14] Abirami, B. S. and E. F. Sundarsingh, "EBG-backed flexible printed Yagi–Uda antenna for on-body communication," *IEEE Transactions on Antennas and Propagation*, Vol. 65, No. 7, 3762–3765, 2017.

[15] Kim, S., Y.-J. Ren, H. Lee, A. Rida, S. Nikolaou, and M. M. Tentzeris, "Monopole antenna with inkjet-printed EBG array on paper substrate for wearable applications," *IEEE Antennas and Wireless Propagation Letters*, Vol. 11, 663–666, 2012.

[16] Cook, B. S. and A. Shamim, "Utilizing wideband AMC structures for high-gain inkjet-printed antennas on lossy paper substrate," *IEEE Antennas and Wireless Propagation Letters*, Vol. 12, 76–79, 2013.

[17] Shah, A. and P. Patel, "Suspended embroidered triangular e-textile broadband antenna loaded with shorting pins," *AEU — International Journal of Electronics and Communications*, Vol. 130, 153573, 2021.

[18] Bait-Suwailam, M. M. and A. Alomainy, "Flexible analytical curve-based dual-band antenna for wireless body area networks," *Progress In Electromagnetics Research M*, Vol. 84, 73–84, 2019.

[19] Alemaryeen, A. and S. Noghanian, "Performance analysis of textile AMC antenna on body model," in *2017 USNC-URSI Radio Science Meeting (Joint with AP-S Symposium)*, 41–42, IEEE, 2017.

[20] Basir, A., A. Bouazizi, M. Zada, A. Iqbal, S. Ullah, and U. Naeem, "A dual-band implantable antenna with wide-band characteristics at MICS and ISM bands," *Microwave and Optical Technology Letters*, Vol. 60, No. 12, 2944–2949, 2018.

[21] IEEE, "IEEE Recommended Practice for Measurements and Computations of Radio Frequency Electromagnetic Fields with Respect to Human Exposure to Such Fields, 100 kHz–300 GHz, Standard IEEE C95.3-2002," 2002.

[22] Commission of European Communities, "Council Recommendation on Limits for Exposure of the Federal Public to Electromagnetic Fields: 0 Hz-300 GHz," 1998.

[23] Hu, X., S. Yan, and G. A. E. Vandenbosch, "Compact circularly polarized wearable button antenna with broadside pattern for U-NII worldwide band applications," *IEEE Transactions on Antennas and Propagation*, Vol. 67, No. 2, 1341–1345, 2018.

[24] Nie, H.-K., X.-W. Xuan, and G.-J. Ren, "Wearable antenna pressure sensor with electromagnetic bandgap for elderly fall monitoring," *AEU — International Journal of Electronics and Communications*, Vol. 138, 153861, 2021.

[25] Keshwani, V. R., P. P. Bhavarthe, and S. S. Rathod, "Compact embedded dual band EBG structure with low SAR for wearable antenna application," *Progress In Electromagnetics Research M*, Vol. 113, 199–211, 2022.

[26] Wang, M., Z. Yang, J. Wu, J. Bao, J. Liu, L. Cai, T. Dang, H. Zheng, and E. Li, "Investigation of SAR reduction using flexible antenna with metamaterial structure in wireless body area network," *IEEE Transactions on Antennas and Propagation*, Vol. 66, No. 6, 3076–3086, 2018.

[27] Kadry, M., M. E. Atrash, and M. A. Abdalla, "Design of an ultra-thin compact flexible dual-band antenna for wearable applications," in *2018 IEEE International Symposium on Antennas and Propagation & USNC/URSI National Radio Science Meeting*, 1949–1950, IEEE, 2018.

[28] Chen, Y.-S. and T.-Y. Ku, "A low-profile wearable antenna using a miniature high impedance surface for smartwatch applications," *IEEE Antennas and Wireless Propagation Letters*, Vol. 15, 1144–1147, 2015.

[29] Gabriel, S., R. W. Lau, and C. Gabriel, "The dielectric properties of biological tissues: III. Parametric models for the dielectric

spectrum of tissues," *Physics in Medicine & Biology*, Vol. 41, No. 11, 2271, 1996.

[30] Kang, K., X. Chu, R. Dilmaghani, and M. Ghavami, "Low-complexity Cole-Cole expression for modelling human biological tissues in (FD) 2TD method," *Electronics Letters*, Vol. 43, No. 3, 143–144, 2007.

[31] Ireland, D. and A. Abbosh, "Modeling human head at microwave frequencies using optimized Debye models and FDTD method," *IEEE Transactions on Antennas and Propagation*, Vol. 61, No. 4, 2352–2355, 2013.

[32] Mersani, A., L. Osman, and J.-M. Ribero, "Performance of dual-band AMC antenna for wireless local area network applications," *IET Microwaves, Antennas & Propagation*, Vol. 12, No. 6, 872–878, 2018.

[33] Joshi, R., E. F. N. M. Hussin, P. J. Soh, M. F. Jamlos, H. Lago, A. A. Al-Hadi, and S. K. Podilchak, "Dual-band, dual-sense textile antenna with AMC backing for localization using GPS and WBAN/WLAN," *IEEE Access*, Vol. 8, 89 468–89 478, 2020.

[34] Vallecchi, A., J. R. D. Luis, F. Capolino, and F. D. Flaviis, "Low profile fully planar folded dipole antenna on a high impedance surface," *IEEE Transactions on Antennas and Propagation*, Vol. 60, No. 1, 51–62, 2011.

[35] Feresidis, A. P., G. Goussetis, S. Wang, and J. C. Vardaxoglou, "Artificial magnetic conductor surfaces and their application to low-profile high-gain planar antennas," *IEEE Transactions on Antennas and Propagation*, Vol. 53, No. 1, 209–215, 2005.

[36] Hosseini, M., A. Pirhadi, and M. Hakkak, "Design of an AMC with little sensitivity to angle of incidence using an optimized Jerusalem cross FSS," in *IEEE International Workshop on Antenna Technology Small Antennas and Novel Metamaterials, 2006.*, 245–248, 2006.

[37] Ali, U., S. Ullah, M. Shafi, S. A. A. Shah, I. A. Shah, and J. A. Flint, "Design and comparative analysis of conventional and metamaterial-based textile antennas for wearable applications," *International Journal of Numerical Modelling: Electronic Networks, Devices and Fields*, Vol. 32, No. 6, e2567, 2019.

[38] Yang, F. and Y. Rahmat-Samii, "Reflection phase characterizations of the EBG ground plane for low profile wire antenna applications," *IEEE Transactions on Antennas and Propagation*, Vol. 51, No. 10, 2691–2703, 2003.

[39] Liu, K., R. Liu, W. Cui, K. Zhang, M. Wang, C. Fan, H. Zheng, and E. Li, "Design of conformal spiral dual-band antenna for wireless capsule system," *IEEE Access*, Vol. 9, 117 349–117 357, 2021.

[40] Kamel, Y. A., H. A. Mohamed, H. ELsadek, and H. M. ELhennawy, "Miniaturized triple-band circular-polarized implantable patch antenna for bio-telemetry applications," *IEEE Antennas and Wireless Propagation Letters*, Vol. 22, No. 1, 74–78, 2022.

[41] Suraj, P. and V. R. Gupta, "Analysis of a rectangular monopole patch antenna," *International Journal of Recent Trends in Engineering*, Vol. 2, No. 5, 106, 2009.

[42] Balanis, C. A., *Antenna Theory: Analysis and Design*, John Wiley & Sons, 2016.